miR-20b promotes growth of non-small cell lung cancer through a positive feedback loop of the Wnt/β-catenin signaling pathway

TAO REN[1*], XING-XING FAN[2*], MEI-FANG WANG[1*], FU-GANG DUAN[2], CHUN-LI WEI[2], RUN-ZE LI[2], ZE-BO JIANG[2], YU-WEI WANG[2], XIAO-JUN YAO[2], MING-WEI CHEN[3], YI-JUN TANG[1] and ELAINE LAI-HAN LEUNG[1,2,4]

[1]Department of Respiratory and Critical Care Medicine, Taihe Hospital, Hubei University of Medicine, Shiyan, Hubei 442000; [2]State Key Laboratory of Quality Research in Chinese Medicine, Macau Institute For Applied Research in Medicine and Health, Macau University of Science and Technology, Taipa, Macau SAR 999078; [3]Department of Respiratory and Critical Care Medicine, The First Affiliated Hospital of Xi'an Jiaotong University, Xi'an, Shanxi 710061; [4]Department of Thoracic Surgery, Guangzhou Institute of Respiratory Health and State Key Laboratory of Respiratory Disease, The First Affiliated Hospital of Guangzhou Medical University, Guangzhou, Guangdong 510000, P.R. China

Received April 20, 2019; Accepted September 4, 2019

DOI: 10.3892/ijo.2019.4940

Abstract. microRNAs (miRNAs or miRs) are endogenous noncoding single-stranded RNA molecules that can regulate gene expression by targeting the 3'-untranslated region and play an important role in many biological and pathological processes, such as inflammation and cancer. In this study, we found that miR-20b was significantly increased in human non-small cell lung cancer (NSCLC) cell lines and patient tissues, suggesting that it may possess a carcinogenic role in lung cancer. This miRNA promoted the proliferation, migration and invasion of NSCLC cells by targeting and downregulating the expression of adenomatous polyposis coli (APC), which is a negative regulator of the canonical Wnt signaling pathway. Wnt signaling activation may increase transcription of miR-20b. Therefore, miR-20b and canonical Wnt signaling were coupled through a feed-forward positive feedback loop, forming a biological regulatory circuit. Finally, an *in vivo* investigation further demonstrated that an increase in miR-20b promoted the growth of cancer cells. Overall, our findings offer evidence that miR-20b may contribute to the development of NSCLC by inhibiting APC via the canonical Wnt signaling pathway.

Correspondence to: Dr Elaine Lai-Han Leung, State Key Laboratory of Quality Research in Chinese Medicine, Macau Institute For Applied Research in Medicine and Health, Macau University of Science and Technology, Room 704b, H building, Avenida Wai Long, Taipa, Macau SAR 999078, P.R. China
E-mail: lhleung@must.edu.mo

Professor Yi-Jun Tang, Department of Respiratory and Critical Care Medicine, Taihe Hospital, Hubei University of Medicine, 32 Renmin South Road, Shiyan, Hubei 442000, P.R. China
E-mail: tangyijun_799@163.com

*Contributed equally

Key words: microRNA-20b, non-small cell lung cancer, Wnt signaling, β-catenin, adenomatous polyposis coli

Introduction

Lung cancer is one of the most common malignancies. In 2012, an estimated 1.8 million new lung cancer cases occurred, accounting for ~13% of total cancer diagnoses cases worldwide (1). Non-small cell lung cancer (NSCLC) accounts for >80% of lung cancer cases and its 5-year survival rate is <15% (2). For these reasons, the elucidation of the molecular mechanisms involved in NSCLC carcinogenesis is important for the identification and development of potential therapeutic targets for NSCLC. At present, increasing evidence has shown that noncoding small RNAs participate in the pathogenesis of NSCLC, providing new perspectives for disease biology.

microRNAs (miRNAs or miRs) are 21-24 nucleotide long small noncoding regulatory RNAs that negatively regulate gene expression at the post-transcriptional and/or translational level by binding to a complementary sequence within the 3'-untranslated regions (UTRs) of target mRNAs (3,4). Approximately one-third to half of human genes are directly regulated by miRNAs and thus, they are associated to a variety of biological processes, including cell proliferation, metastasis, differentiation and apoptosis, which are important in the development of cancer (5). Abnormal changes in miRNA expression have been reported to be closely associated with cancer initiation and progression, and therefore, these molecules are key oncogenes or tumor suppressor genes in NSCLC (6-8).

miR-20b is located on human chromosome X, encoded by the miR-106a-363 cluster and divided into miR-17 family members based on the degree of homology of the seed sequence (9). Numerous studies have shown the different roles of miR-20b in various types of cancer. For example, miR-20b

was reduced in papillary thyroid carcinoma (10) and renal cell carcinoma (11), showing its tumor-suppressor function. In contrast, the carcinogenic potential of miR-20b has been demonstrated in breast cancer (12), esophageal cancer (13), colorectal cancer (14) and T-cell leukemia (15). However, the biological functions of miR-20b in NSCLC remain poorly understood.

The Wnt/β-catenin signaling pathway is involved in various biological processes, such as cell proliferation, movement, differentiation and cell death, which are necessary for cell development and morphology (16-18). When β-catenin enters the cell nucleus, it can regulate target gene transcription by interacting with the transcription factor lymphoid enhancer-binding factor 1/T cell-specific transcription factor. These target genes, such as cyclin D1 and c-myc, are significant for cell differentiation, proliferation and apoptosis (19-21)

The purpose of this study was to clarify the biological function of miR-20b and its role in regulating Wnt signaling in NSCLC. The findings revealed that miR-20b regulates the canonical Wnt signaling pathway in NSCLC cells to promote proliferation. In addition, we observed that miR-20b activated Wnt signaling by reducing adenomatous polyposis coli (APC) expression. These results elucidated a new mechanism for excessive activation of the Wnt/β-catenin signaling pathway in NSCLC and miR-20b may be a potential therapeutic target for lung cancer.

Materials and methods

Cell culture and transfection. Lung adenocarcinoma cell lines (PC-9, H1975 and A549), a non-small cell lung cancer line (H1299), a normal lung epithelial cell line (BEAS-2B) were purchased from the American Type Culture Collection. PC-9, H1975, A549 and H1299 were cultured in RPMI-1640 (Gibco; Thermo Fisher Scientific, Inc.). BEAS-2B cells were cultivated in Bronchial Epithelial Cell Basal medium (BEBM; Lonza Group, Ltd.). All culture media were supplemented with 10% fetal bovine serum (FBS; Invitrogen; Thermo Fisher Scientific, Inc.) with 100 U/ml penicillin and 100 μg/ml streptomycin (Invitrogen; Thermo Fisher Scientific, Inc.). All cells were cultivated at 37˚C in a 5% CO_2 incubator.

Information of the cell lines is as detailed by the supplier as follows: i) BEAS-2B cells were derived from normal bronchial epithelium obtained from autopsy of noncancerous individuals. Cells were infected with a replication-defective SV40/adenovirus 12 hybrid and cloned; ii) PC-9 was originally deposited with the Riken BioResource Center as a cell line derived from human lung adenocarcinoma (undifferentiated type) in 1989; iii) H-1975 is an adenocarcinoma, non-small cell lung cancer cell line; iv) A-549 are adenocarcinoma human alveolar basal epithelial cells and the cell line was developed in 1972 through the removal and culturing of cancerous lung tissue in the explanted tumor of a 58-year-old Caucasian male; and v) H1299 are carcinoma, non-small cell lung cancer cells.

Transfection. miRNA mimics, inhibitors and negative controls were synthesized by Shanghai GenePharma Co., Ltd. and transfection was performed with Lipofectamine™ LTX Reagent (Invitrogen; Thermo Fisher Scientific, Inc.). A total of $1.5x10^5$ PC-9 or H1975 cells per well were seeded in 6-well plates 24 h prior to transfection. The transfection reaction contained 100 μM miRNA diluted in 100 μl Opti-MEM® I Reduced Serum Medium (Invitrogen; Thermo Fisher Scientific, Inc.). Next, 4 μl LTX reagent was added to each sample and incubated for 5-15 min at room temperature. Finally, the transfection mixture was added to the cells and mixed gently. After 48 h, expression levels were detected by reverse transcription-quantitative (RT-q) PCR.

Cell viability assay. Cells were seeded at 5,000 cells per well in 96-well plates at 24 h after transfection. The MTT assay was used to determine cell viability at 24, 48, 72 and 96 h after the cells were seeded. Briefly, 20 μl of MTT dye solution (5 mg/ml) was added to each well and continually incubated for 4 h. Then, the supernatant was removed and 150 μl of DMSO was added to stop the reaction. The absorbance at 490 nm was measured.

The results were confirmed by manual cell counts. Here, transfected cells were seeded in 24-well plates at 10,000 cells per well, collected at 24, 48, 72 and 96 h and counted using a hemocytometer.

Colony formation assay. After transfection with miR-20b mimics and inhibitors for 48 h, cells were plated in 6-well plates at 5,000 per well and grown for 2 weeks. After 2 weeks, the colonies were washed 3 times with cold PBS, fixed with 4% paraformaldehyde for 20 min and then cells were washed twice with PBS and fixed with methanol/acetic acid (3:1, v/v) for 15 min at room temperature. Then, they were stained with 0.5% crystal violet for 30 min at room temperature. The number of colonies was counted under a light microscope (magnification, x4).

Wound healing assay. Scratch wound assays were performed to evaluate the motility of the cells at 24 h after transfection. A total of $2x10^5$ cells per well were seeded in 6-well plates. At 90-95% confluence, the monolayer of cells was scratched with a 10 μl micropipette tip. After removal of cellular debris, the cultures were incubated in RPMI 1640 for 24 h, and recovery of the wound was observed and photographed with a light microscope (magnification, x10).

Migration and invasion assays. For the Transwell assays, 8-μm pore size chambers (Corning, Inc.) were used with an insert without (migration) or with (invasion) Matrigel coating (BD Biosciences). At 24 h after transfection, $1x10^5$ cells in serum-free medium were added to the upper chamber. The lower chamber was filled with 10% FBS RPMI 1640. After 24-h incubation, cells remaining on the upper surface of the membrane were removed, whereas cells that had invaded through the membrane were fixed with 0.1% paraformaldehyde for 20 min at room temperature, stained with 0.1% crystal violet for 30 min at room temperature, imaged and counted under a light microscope (magnification, x10).

Nuclear isolation. The nuclear fraction was extracted with the nuclear extraction kit (Thermo Fisher Scientific, Inc.). Briefly, $5x10^6$ transfected cells were gently suspended in 500 μl Hypotonic Buffer by pipetting up and down and incubated on ice for 15 min. Then, 25 μl detergent (10% NP40) was added

and vortexed for 10 sec at the highest setting at room temperature. The homogenate was centrifuged for 10 min at 3,000 x g at 4˚C. The supernatant was the cytoplasmic and the pellet the nuclear fraction.

Immunofluorescence. After treatment, cells were fixed with 0.1% paraformaldehyde for 20 min at room temperature. The fixed cells were blocked with 5% BSA (Sigma-Aldrich; Merck KGaA) at room temperature for 2 h and then incubated with anti-β-catenin primary antibody (1:1,000; cat. no. 8480; Cell Signaling Technology, Inc.) overnight at 4˚C. After washing with PBS at room temperature three times (5 min/each), Goat anti-rabbit fluorescence conjugated second antibody (1:10,000; cat. no. A21245; Invitrogen; Thermo Fisher Scientific, Inc.) was added for 1 h at room temperature and imaged using a confocal microscope (magnification, x60).

Western blot analysis. Transfected cells were lysed in RIPA lysis buffer with protease and phosphatase inhibitors (Roche Applied Science.) to extract the total protein. The concentration of the total protein extract was determined with a DCTM Protein Assay kit (Bio-Rad Laboratories, Inc.). Then, 40 μg total protein lysate were separated on 10% SDS-PAGE gels and transferred to a nitrocellulose membrane. Membranes were blocked with 5% non-fat milk in TBST (5% Tween-20) for 1 h at room temperature. Primary antibodies, including anti-APC (cat. no. 2504), anti-β-catenin (cat. no. 8480), anti-c-Myc (cat. no. 18583), anti-cyclin D1(cat. no. 2978), GAPDH (cat. no. 5174) and lamin B (cat. no. 12586), which were all purchased from Cell Signaling Technology, Inc, were incubated with the membranes at 1:1,000 dilution overnight at 4˚C. After the membrane was washed with TBST (3x5 min), fluorescent-conjugated goat anti-rabbit (cat. no. 926-32211; 1:10,000; LI-COR Biosciences) or goat anti-mouse secondary antibodies (cat. no. 926-32210; 1:10,000; LI-COR Biosciences) was added to the membrane at room temperature for 1 h. GAPDH and lamin B were used as loading controls for cellular and nuclear proteins, respectively. The signal intensity of the membranes was detected with an Odyssey Scanner (LI-COR, Inc.).

Isolation of human plasma. Human healthy and lung cancer plasma specimens (20 each) were obtained following the guidelines approved by the institutional review board at Taihe Hospital of Hubei University of Medicine, and written informed consent was obtained from patients in all cases. A total of 40 subjects were enrolled in this study, including 20 NSCLC patients (age, 57.3±9.1 years; male, 14; female, 6) between January 2018 and July 2018, of which 11 patients had tumor resection (stages I, II and IIIA) and 9 patients did not (stages IIIB and IV), and 20 age- and sex-matched healthy volunteers as controls (age, 54.1±9.2 years; male, 15; female, 5; P=0.081). NSCLC patients were recruited at Department of Respiratory and Critical Care Medicine, Taihe Hospital of Hubei University of Medicine, China. Blood samples were taken before chemotherapy in both operable and non-operable patients. There were no other inclusion or exclusion criteria for this study. Tumors were staged according to the tumor-node-metastasis (TNM) staging system of the American Joint Committee on Cancer (1). None of the patients had received adjuvant chemotherapy or radiotherapy before admission. Informed consents were obtained from all enrolled subjects and the local Ethics Committee approved the protocol.

RNA extraction. miRNA was extracted with mirVana™ miRNA extraction kit (Invitrogen; Thermo Fisher Scientific, Inc.) according to the manufacturer's instructions. Briefly, after the medium was removed, 0.6 ml lysis buffer with 1% 2-mercaptoethanol was added to the $1x10^6$ cells. The total cell lysate was transferred to an RNase-free tube and the cell pellet was dispersed. One volume of 70% ethanol was added to the cell lysate and mixed thoroughly to disperse visible precipitate. The mixture was transferred to a spin cartridge, centrifuged at 12,000 x g for 15 sec at room temperature and the flow-through was discarded. The spin cartridge was washed with wash buffer I and buffer II, and RNA was eluted with 50 μl of RNase-free water. The RNA concentration was determined and RNA quality was assessed by agarose (1%) electrophoresis.

cDNA synthesis. The synthesis of first-strand cDNA was carried out following the instructions of the Transcriptor First Strand cDNA synthesis kit (Roche Diagnostics). DNase-treated RNA (1 μg) was used in the synthesis reaction. The RNA sample was incubated with 2 μl random and 1 μl Oligo (dT) primers (with kit) at 65˚C for 10 min and then cooled on ice for 2 min. The reaction mixture, containing reaction buffer, RNase inhibitor and reverse transcriptase, was added to the tube and incubated at 25˚C for 10 min followed by 55˚C for 30 min. The reaction was terminated by heating to 70˚C for 15 min. cDNA was stored at -80˚C until further use. Primers were designed as follows: U6 for reverse transcription (RT), 5'-GTCGTATCC AGTGCAGGGTCCGAGGTGCACTGGATACGACAAAAT ATGGAAC-3'; and miR-20b for RT, 5'-GTCGTATCCAGT GCAGGGTCCGAGGTGCACTGGATACGACCTACCTG-3'.

Quantitative (q) PCR. qPCR was performed using FastStart Universal SYBR Green Master Mix (Roche Applied Science). The reaction mixture contained 10 μl SYBR Master mix, 1 μl forward and reverse primers, 0.2 μl template and water to 20 μl. The PCR protocol was 94˚C for 10 min, followed by 40 cycles of 94˚C for 10 sec and 60˚C for 30 sec. U6 and β-actin were used as references for normalization of the expression of miRNA and mRNAs, respectively, and the $2^{-\Delta\Delta Cq}$ method was used to determine the relative expression of each transcript (22). Experiments were repeated at least three times. The RT-qPCR primers were as follows: U6, forward, 5'-TGC GGGTGCTCGCTTCGGCAGC-3 and reverse, 5'-CCAGTG CAGGGTCCGAGGT-3'; miR-20b, forward, 5'-GCCCGC CAAAGTGCTCATAGTG-3' and reverse, 5'-CCAGTGCAG GGTCCGAGGT-3'; β-actin, forward, 5'-TCACCCACACTG TGCCCATCT-3' and reverse, 5'-GTGAGGATCTTCATG AGGTAGTCAGTC-3'; and APC, forward, 5'-AAGCGTATT GAGTGCCTTATGG-3' and reverse, 5'-GGTAAGTAAGAG TGCCAACCAA-3'.

$A549^{\beta\text{-catenin}(-/-)}$ CRISPR-Cas9 sgRNA design and sgRNA cloning. The study was based on Cas9, which was used to target the PAM sequence on β-catenin. The two targeting sequences used to knock out β-catenin were GGACTCTGGAATCCATTCTG and

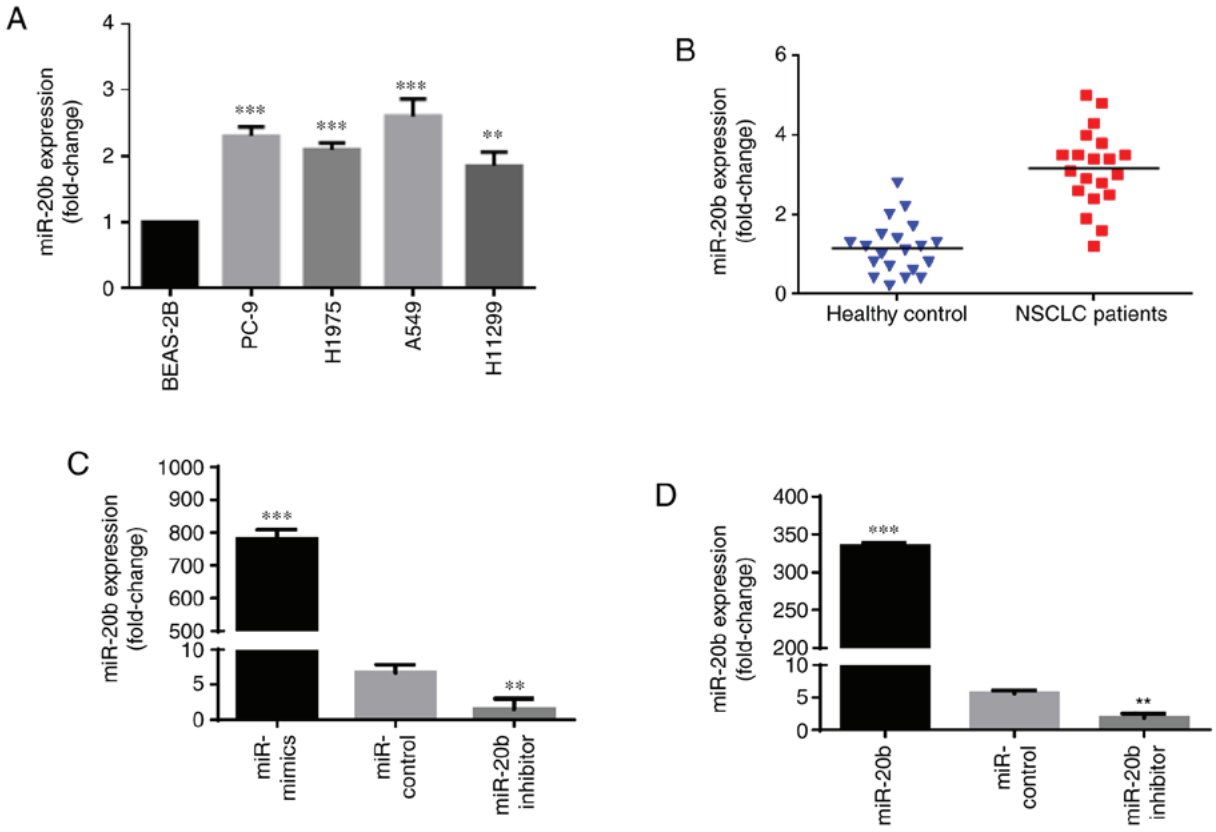

Figure 1. miR-20b is increased in NSCLC cell lines and clinical samples. (A) Relative expression level of miR-20b in NSCLC cell lines, PC-9, H1975, A549 and H1299, and in BEAS-2B cells determined by RT-qPCR. **P<0.01 and ***P<0.001 vs. BEAS-2B. (B) Expression level of miR-20b in the plasma of NSCLC patients (n=20) and healthy donors (n=20) determined by RT-qPCR. miR-20b expression detected by RT-qPCR in (C) PC-9 and (D) H1975 NSCLC cells transfected with miR-20b mimics, miR-20b inhibitor or associated controls. **P<0.01 and ***P<0.001 vs. miR-control. Data are presented as the mean ± SEM. RT-qPCR, reverse transcription-quantitative PCR; miR, microRNA; NSCLC, non-small cell lung cancer.

ACCACAGCTCCTTCTCTGAGAG. DNA oligos were synthesized and cloned into pX335-U6-Chimeric_BB-CBh-hSpCas9n (D10A) (cat. no. 42335; Addgene, Inc.). The vector was transfected into A549 cells using Lipofectamine™ 2000 (Invitrogen; Thermo Fisher Scientific, Inc.). The β-catenin knockout cell line comes from our latest publication (23).

Tumor xenograft model. Animal studies were approved by the Ethical Committee of Macau University of Science and Technology. BALB/c Nude mice (n=16; age, 6-8 weeks) were maintained under specific pathogen-free conditions and housed in plastic cages in groups of four. Each group contained 8 mice. The housing conditions of the animals were as follows: Temperature 22±1˚C, humidity 40-60%, 12-h dark/light cycles and free access to food and water. miR-20b-overexpressing H1975 cells and empty vector control cells cultured in RPMI-1640 were harvested, washed with PBS and re-suspended in medium. A total of $1x10^6$ cells/100 μl were mixed with 50 μl Matrigel and injected subcutaneously into the right forelimb of each nude mouse. Tumor volume was measured using a caliper every 7 days and calculated using the following equation: Volume = ($width^2$ x length)/2. At 28 days after inoculation, mice were sacrificed and tumor weights were assessed.

Statistical analyses. All data are expressed as the mean ± SEM of three individual experiments. Differences between groups were determined using one-way ANOVA followed by Bonferroni's test using GraphPad Prism 5 (GraphPad Software, Inc.) or by paired Student's t-test was used to compare two groups. The level of significance was set at P<0.05.

Results

miR-20b is significantly upregulated in NSCLC cell lines. To determine the role of miR-20b in NSCLC, we first investigated and compared its expression in a normal lung epithelial cell line, BEAS-2B, and different types of NSCLC cell lines, namely PC-9, H1975, A549 and H1299. The results showed that the levels of miR-20b in PC-9, H1975, A549 and H1299 were significantly higher than that in BEAS-2B (Fig. 1A). Moreover, we compared miR-20b expression in clinical NSCLC samples and healthy donor samples. By analyzing the miR-20b expression levels in the plasma of 20 healthy donors and 20 NSCLC patients, we found that the plasma level of miR-20b was increased in the NSCLC patients (Fig. 1B), which is consistent with the results of the cell lines. Taken together, these data indicated that miR-20b was increased in NSCLC cells and tissues and may act as an oncogene.

miR-20b enhances proliferation, migration and invasion of NSCLC cells. Since the EGFR mutation is a dominant mutation in NSCLC (24), we chose PC-9 ($EGFR^{exon19del\ E746–A750}$) and H1975 ($EGFR^{L858R+T790M}$) for further experiments. miR-20b

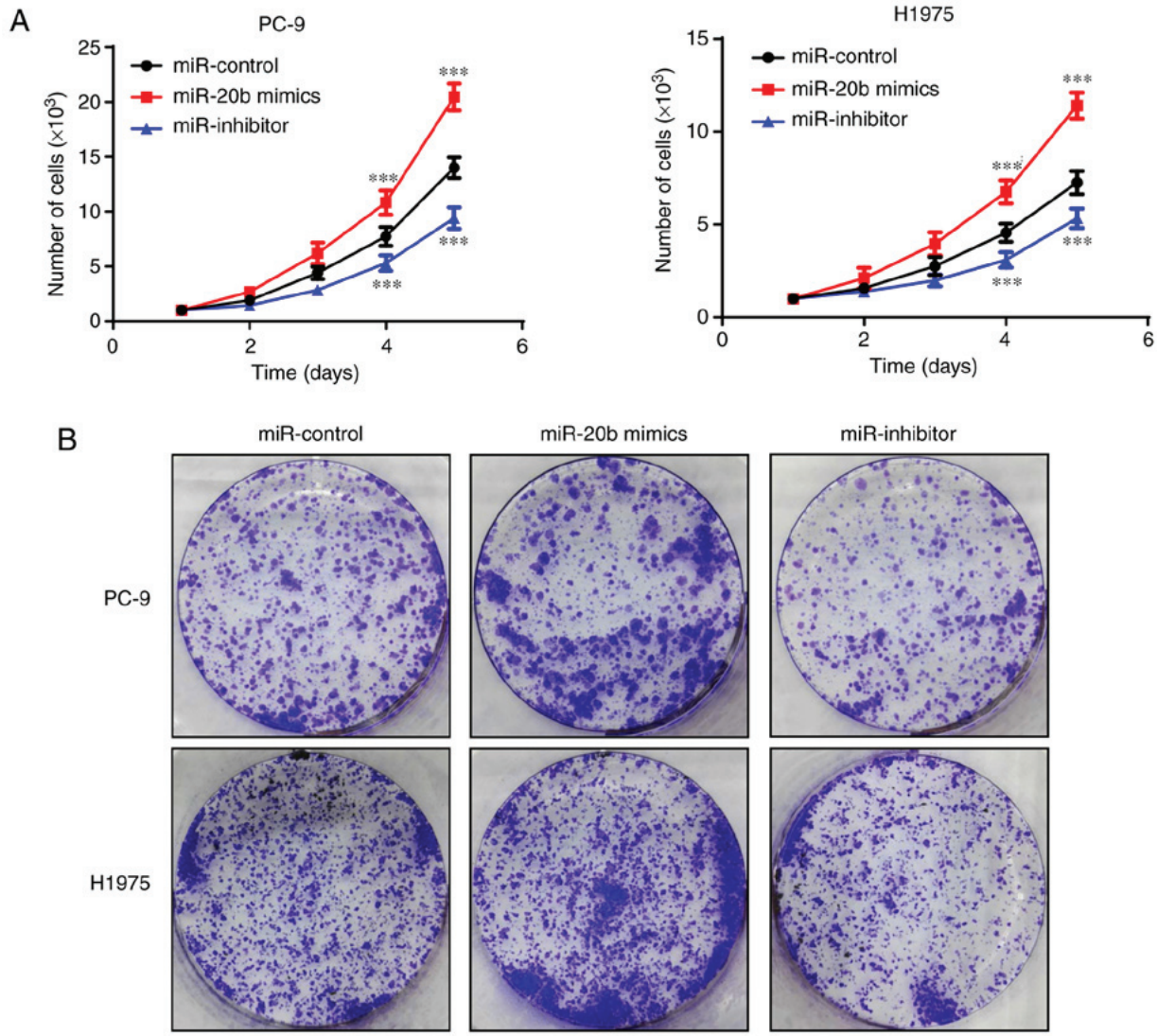

Figure 2. miR-20b enhances proliferation of non-small cell lung cancer cells. (A) Growth curves of PC-9 and H1975 transfected with miR-20b mimics, miR-20b inhibitor and miR control. (B) Colony formation assays for PC-9 and H1975 cells transfected with miR-20b mimic, miR-20b inhibitor or miR control. ***P<0.001 vs. miR control. miR, microRNA.

inhibitors, mimics and negative control were transfected into PC-9 and H1975. Transfection efficiency was measured by RT-qPCR and compared with the miR-NC, miR-20b expression was significantly increased in the presence of the mimics and significantly downregulated in the presence of miR-20b inhibitors in PC-9 and H1975 (Fig. 1C and D).

To investigate whether miR-20b acted as an oncogene in NSCLC, cellular function assays were performed after transfection. First, growth curves and colony formation assays were applied to assess cell proliferation. As shown in Fig. 2, an increasing level of miR-20b was associated with the cell proliferation rate. Increased miR-20b levels in PC-9 and H1975 significantly enhanced the proliferative capacity, and decreased miR-20b levels significantly suppressed cell growth in PC-9 and H1975.

Next, we used wound healing and Transwell assays to investigate the effect of miR-20b on the migration and invasion of NSCLC cells. Overexpression of miR-20b markedly promoted wound closure compared with the control in PC-9 and H1975 cells, whereas miR-20b inhibitor treatment reduced cell migration (Fig. 3A and B). Similar results were observed in the migration and invasion assays. Using Transwell assays with or without Matrigel, we found that in cells with increased miR-20b expression, the number of invasive and migrated cells increased, while miR-20b inhibitors had the opposite effect on NSCLC cells (Fig. 3C and D).

In summary, the above data suggested that overexpression of miR-20b promoted cell proliferation, migration and invasion in NSCLC cells, whereas miR-20b inhibitors reduced these functions.

miR-20b promotes the Wnt signaling pathway through regulating APC. As miR-20b was demonstrated to be beneficial in promoting NSCLC growth *in vitro*, we further explored its role as an oncogene. Previous reports on other types of cancer showed that APC is a downstream target of miR-20b (25). We detected and compared APC expression in normal lung epithelial cells and NSCLC cell lines. As shown in Fig. 4A, APC mRNA in PC-9, H1975, A549 and H1299 was significantly lower than in normal lung BEAS-2B cells and APC protein

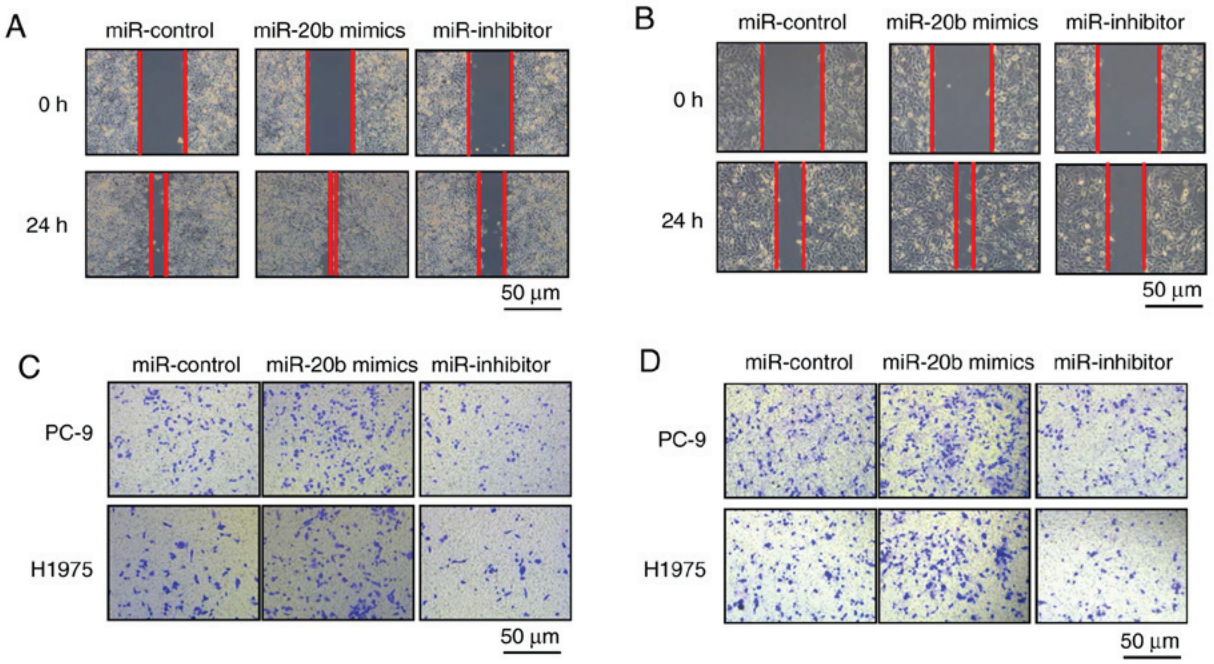

Figure 3. miR-20b promotes migration and invasion of non-small cell lung cancer cells. Wound closure at 0 and 24 h in (A) PC-9 and (B) H1975 cells transfected with miR-20b mimic, miR-20b inhibitor or miR-control; scale bar, 100 μm. Transwell (C) migration and (D) invasion assays of PC-9 and H1975 cells transfected with miR-20b mimic, miR-20b inhibitor or miR-control; scale bar, 100 μm. miR, microRNA.

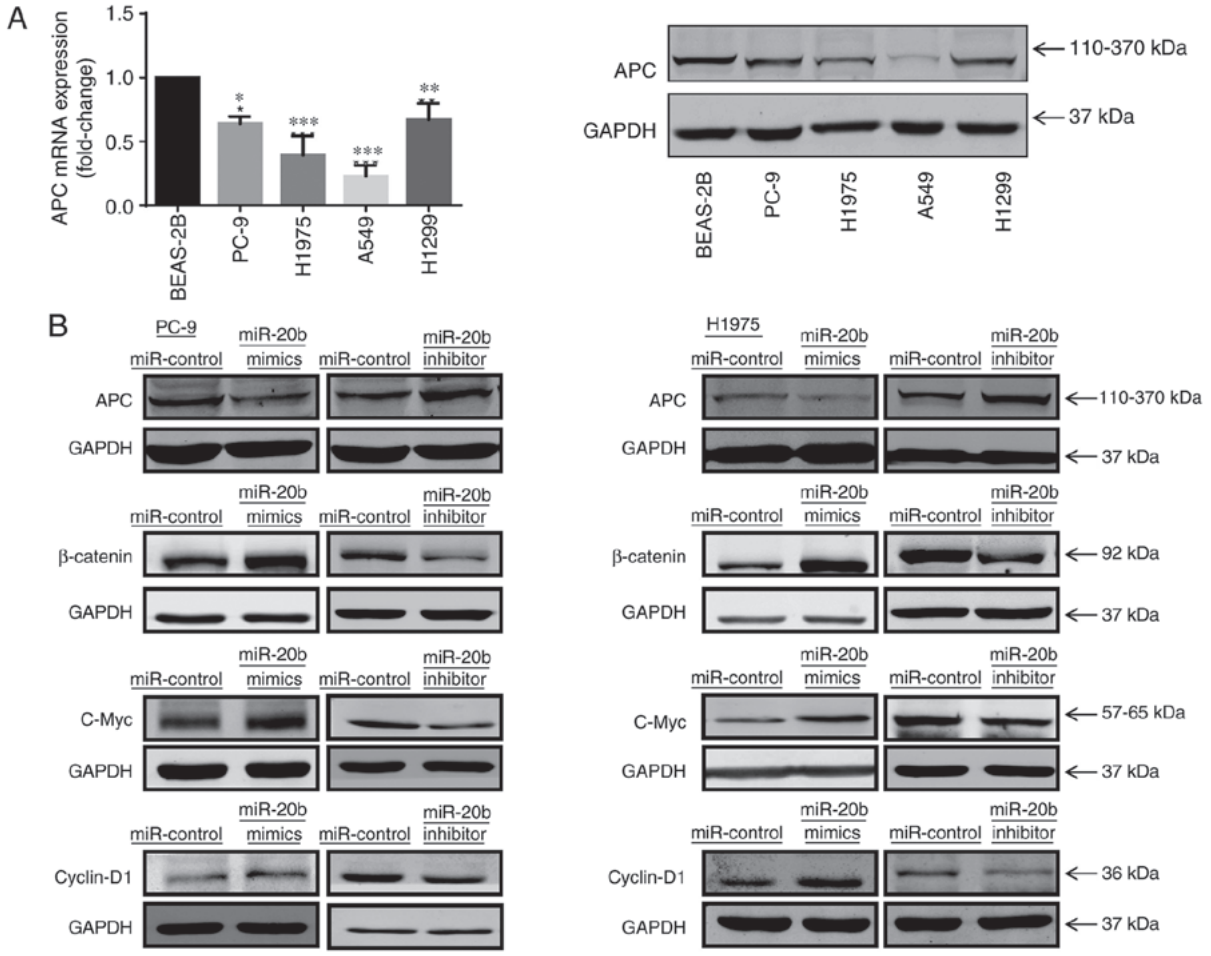

Figure 4. miR-20b activates the Wnt/β-catenin signaling pathway. (A) Relative mRNA and protein expression levels of APC in non-small cell lung cancer cell lines, PC-9, H1975, A549 and H1299, and BEAS-2B cells. *P<0.05, **P<0.01 and ***P<0.001 vs. BEAS-2A. (B) Western blot analysis of APC, β-catenin, C-Myc and cyclin D1 expression in PC-9 and H1975 cells transfected with miR-20b mimics, miR-20b inhibitor or miR-NC. miR, microRNA; NC, negative control; APC, adenomatous polyposis coli.

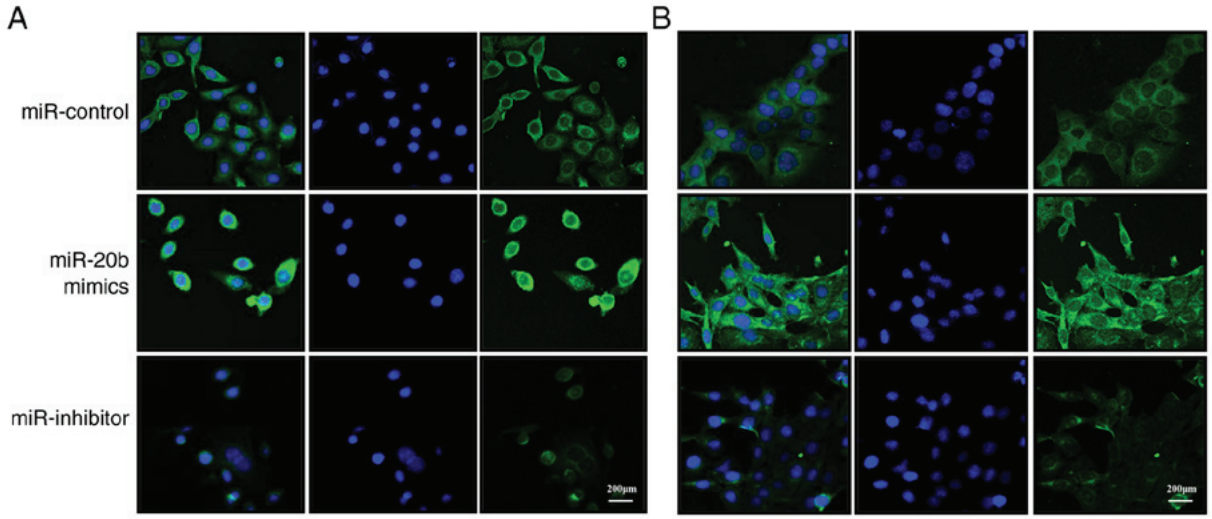

Figure 5. β-catenin expression is regulated by miR-20b. β-catenin expression in (A) PC-9 and (B) H1975 transfected with miR-20b mimic, miR-20b inhibitor or miR-control was observed using immunofluorescence imaging; β-catenin in green and nuclei in blue; scale bar, 200 μm. miR, microRNA.

levels were also changed. Additionally, we determined APC levels in cells transfected with miR-20b mimics to increase and miR-20b inhibitors to decrease miR-20b expression. Protein levels of APC were decreased in mimic-treated and increased in inhibitor-treated cells compared with the respective controls (Fig. 4B). These data suggested that miR-20b affected the expression of APC.

APC is a negative regulator of the Wnt/β-catenin signaling pathway, which is an essential factor in cancer growth and metastasis (7). To identify whether miR-20b promotes cancer through Wnt signaling transduction, we detected the levels of β-catenin in NSCLC cells transfected with miR-20b mimics and inhibitors. As depicted in Fig. 4B, a marked increase of β-catenin was detected in PC-9 and H1975 cells transfected with miR-20b mimic, whereas the miR-20b inhibitor decreased β-catenin compared with the respective controls. Immunofluorescence confocal imaging showed an increase in the β-catenin protein expression in PC-9 and H1975 cells overexpressing miR-20b, while transfection with miR-20b inhibitors decreased expression compared with the control (Fig. 5). The translocation of β-catenin to the nucleus was enhanced by miR-20b overexpression (Fig. S1).

In addition, we explored the effects of miR-20b overexpression and knockdown on c-Myc and cyclin D1, which are downstream target genes of the Wnt/β-catenin signaling pathway in cancer (26,27). As shown in Fig. 4B, protein levels of these genes increased in PC-9 and H1975 overexpressing miR-20b and decreased in inhibitor-treated cells compared with the controls. These findings suggested that miR-20b enhanced the expression of β-catenin and activated Wnt/β-catenin downstream signaling in NSCLC cells.

miR-20b modulates the Wnt/β-catenin signaling pathway in tumorigenesis through a positive feedback loop. To investigate the association between β-catenin and miR-20b, we examined miR-20b expression in three different samples, namely $A549^{WT}$, $A549^{\beta\text{-catenin}(-/-)}$ and A549 treated with Wnt inhibitor. The results demonstrated a significantly higher expression of miR-20b and a significantly increased level of APC in $A549^{WT}$ cells compared with $A549^{\beta\text{-catenin}(-/-)}$ and A549 cells treated with Wnt inhibitor (Fig. 6A). These assays demonstrated that β-catenin induced miR-20b transcription, and in turn, miR-20b activated the Wnt/β-catenin signaling pathway. Thus, it was suggested that miR-20b and Wnt signaling may be coupled through a forward-positive feedback loop and form a biological regulatory circuit.

miR-20b promotes tumor growth in vivo. To further classify the function of miR-20b in NSCLC tumor growth, we used established an *in vivo* xenograft mouse model. H1975 overexpressing miR-20b and control cells were injected subcutaneously into the right forelimb of the mice. As shown in Fig. 6B and C, the tumor weight and volume for animals injected with miR-20b-overexpressing cells were significantly higher than those of the control group. These results confirmed that miR-20b promoted tumor growth of H1975 cells transfected with miR-20b *in vivo.*

Discussion

miR-20b levels were reported to be significantly higher in serum exosomes from patients with NSCLC at more advanced stages of disease and the presence of lymph node metastases than in healthy controls, suggesting that miR-20b might be a promising biomarker for the diagnosis of lung cancer (28). In our study, evidence for a new mechanistic link between miR-20b and the Wnt/β-catenin signaling pathway was suggested for NSCLC cells (Fig. 6D). We discovered that miR-20b was markedly upregulated in NSCLC cell lines and in clinical NSCLC samples. *In vitro* and *in vivo*, miR-20b overexpression accelerated cancer progression, but miR-20b downregulation suppressed the growth and metastasis of NSCLC cells *in vitro.* In addition, we confirmed that miR-20b regulated the expression of APC, a key negative regulator of the Wnt/β-catenin signaling pathway, leading to activation of the Wnt/β-catenin signaling pathway. Taken together, our findings suggested that miR-20b may function as an onco-miR and may be considered a key target for clinical treatment in NSCLC.

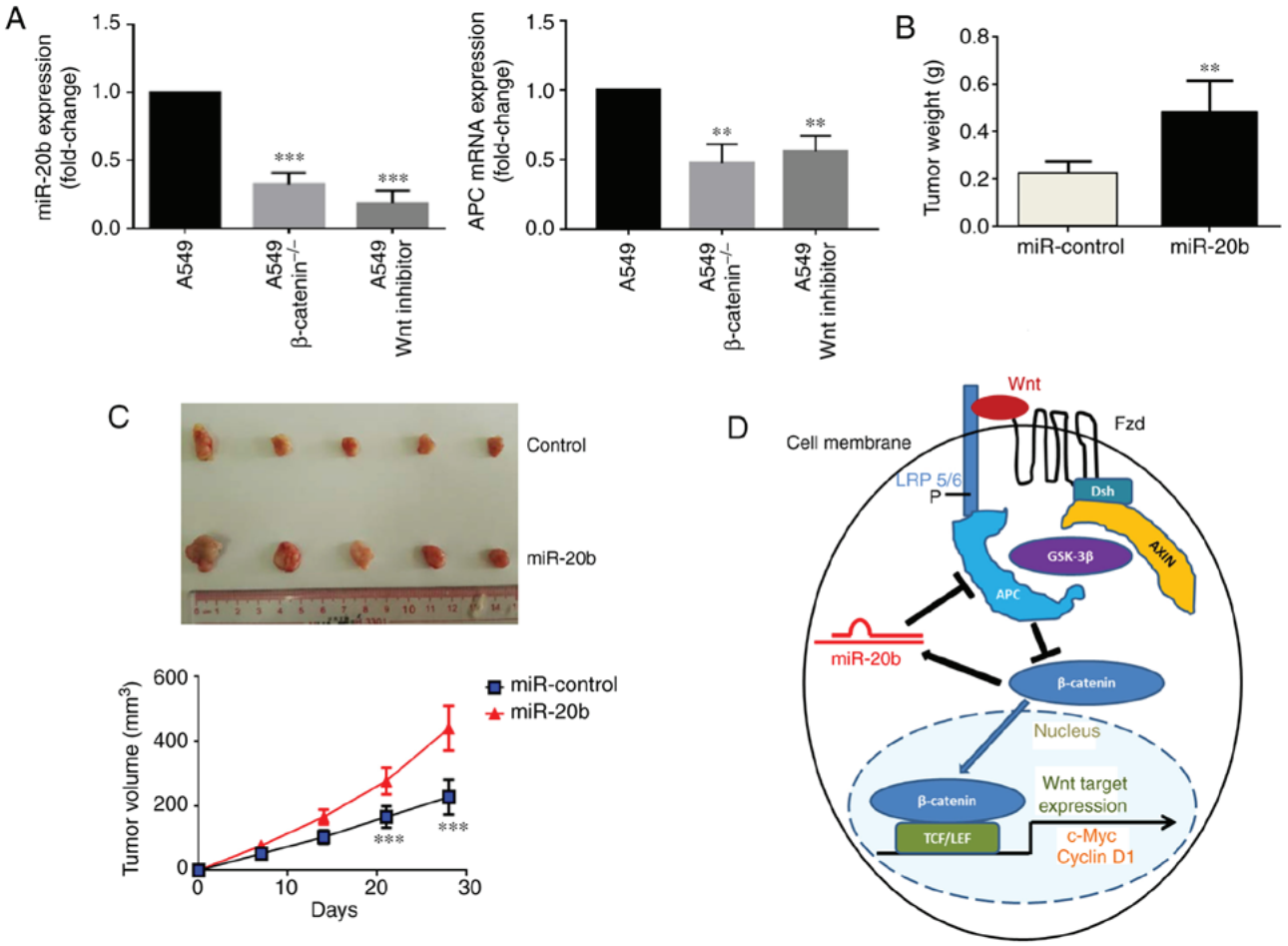

Figure 6. miR-20b promotes tumor growth of H1975 *in vivo*. (A) Relative expression levels of miR-20b and APC in A549 (wild type), A549$^{\beta\text{-catenin}(-/-)}$ and A549 Wnt inhibitor cells determined by reverse transcription-quantitative PCR. **P<0.01 and ***P<0.001 vs. A549. Tumor (B) weight and (C) volume of xenograft tumors derived from nude mice (n=8 per group) injected with control or miR-20b-overexpressing H1975 cells after 28 days. As some of the samples were damaged during the excision process, 5 specimens from each group were presented. **P<0.01 and ***P<0.001 vs. miR-control. (D) Cell model of the miR-20b mechanism of action. miR, microRNA; APC, adenomatous polyposis coli; P, phosphate; Fzd, frizzled; Dsh, dishevelled; AXIN, axis inhibition protein; GSK-3β, glycogen synthase kinase 3β; TCF/LEF, T-cell factor/lymphoid enhancer-binding factor; LRP, lipoprotein receptor-related proteins.

Activation of the Wnt/β-catenin signaling pathway is commonly observed in many types of human malignancy and is considered to promote cancer progression (29-31). APC has been found to be inhibited in cancer, which helps to promote cancer progression via regulation of the oncogenic Wnt/β-catenin signaling pathway. For instance, in human hepatoma cells, miR-106b activated canonical Wnt signaling to enhance cancer progression by directly targeting APC (32). Downregulation of miR-129-5p inhibits growth and induces apoptosis in laryngeal squamous cell carcinoma by targeting APC (33). In addition, the loss of APC function in a mouse model leads to hyper-activation of Wnt/β-catenin signaling and causes colorectal cancer (34). Mice with a heterozygous truncated APC mutant exhibit enhanced Wnt/β-catenin signaling activity and develop mammary adenocarcinomas and subsequent pulmonary metastases (35). Here, we showed that miR-20b inhibited APC expression, which was consistent with the tumor suppressor effect of APC. Overexpression of miR-20b in NSCLC cell lines significantly promoted the proliferation of NSCLC *in vitro* and *in vivo*. Our research revealed a potentially novel mechanism of the miR-20b/APC axis in NSCLC.

Based on the impact of Wnt/β-catenin signaling on cancer progression, anticancer drugs targeting the Wnt/β-catenin signaling pathway have attracted much attention (36). However, most Wnt signaling genes mutated in colorectal cancer, including APC, are tumor suppressors and cannot be directly targeted for therapeutic purposes (37). β-catenin is a proto-oncogene that is a ubiquitously expressed cell adhesion molecule and cannot be used as a drug target (37). Therefore, finding new molecules that play an important role in the inactivation of the Wnt/β-catenin signaling pathway has clinical application potential.

In summary, the results of the present study indicated for the first time that miR-20b and Wnt signaling were coupled through a feed-forward positive feedback loop, forming a biological regulatory circuit. Our results provided evidence that miR-20b promoted NSCLC partially by inhibiting APC and the findings uncover a novel mechanism of Wnt/β-catenin signaling pathway hyper activation in NSCLC. However, there are limitations to this study, including the status of miR-20b and APC in tumor tissue remains unknown. To validate this potential target in the future, the difference between primary lung tumor tissues and adjacent non-tumor tissues could be examined.

Acknowledgements

Not applicable.

Funding

This work was supported by FDCT grants from the Science and Technology Development Fund of Macao (grant nos. 003/2018/A1, 130/2017/A3 and 046/2016/A2) and the Scientific and Technological Project of Shiyan City of Hubei Province of China (grant no. ZD2013014).

Availability of data and materials

All the datasets generated and analyzed in the present study are included in this published article.

Authors' contributions

ELHL, YJT and MWC conceived the study. ELHL and YJT designed the experiments and supervised all research. TR, XXF and MFW carried out the experiments and prepared the draft of the manuscript. FGD, CLW and RZL performed the animal study. ZBJ, YWW and XJY analyzed the data. All authors read and approved the final manuscript.

Ethics approval and consent to participate

Human lung cancer tissue specimens were obtained following the guidelines approved by the institutional review board at Taihe Hospital of Hubei University of Medicine, and written informed consent was obtained from patients in all cases. Animal studies were approved by the Ethical Committee of Macau University of Science and Technology.

Patient consent for publication

Not applicable.

Competing interests

The authors declare that they have no competing interests.

References

1. Torre LA, Bray F, Siegel RL, Ferlay J, Lortet-Tieulent J and Jemal A: Global cancer statistics, 2012. CA Cancer J Clin 65: 87-108, 2015.
2. Fassina A, Cappellesso R and Fassan M: Classification of non-small cell lung carcinoma in transthoracic needle specimens using microRNA expression profiling. Chest 140: 1305-1311, 2011.
3. Bartel DP: MicroRNAs: Genomics, biogenesis, mechanism, and function. Cell 116: 281-297, 2004.
4. Lewis BP, Burge CB and Bartel DP: Conserved seed pairing, often flanked by adenosines, indicates that thousands of human genes are microRNA targets. Cell 120: 15-20, 2005.
5. Schepeler T: Emerging roles of microRNAs in the Wnt signaling network. Crit Rev Oncog 18: 357-371, 2013.
6. Zhang T, Hu Y, Ju J, Hou L, Li Z, Xiao D, Li Y, Yao J, Wang C, Zhang Y and Zhang L: Downregulation of miR-522 suppresses proliferation and metastasis of non-small cell lung cancer cells by directly targeting DENN/MADD domain containing 2D. Sci Rep 6: 19346, 2016.
7. Stoddart A, Wang J, Hu C, Fernald AA, Davis EM, Cheng JX and Le Beau MM: Inhibition of WNT signaling in the bone marrow niche prevents the development of MDS in the Apc$^{(del/+)}$ MDS mouse model. Blood 129: 2959-2970, 2017.
8. Iqbal MA, Arora S, Prakasam G, Calin GA and Syed MA: MicroRNA in lung cancer: Role, mechanisms, pathways and therapeutic relevance. Mol Aspects Med 70: 3-20, 2019.
9. Mendell JT: miRiad roles for the miR-17-92 cluster in development and disease. Cell 133: 217-222, 2008.
10. Hong S, Yu S, Li J, Yin Y, Liu Y, Zhang Q, Guan H, Li Y and Xiao H: miR-20b displays tumor-suppressor functions in papillary thyroid carcinoma by regulating the MAPK/ERK signaling pathway. Thyroid 26: 1733-1743, 2016.
11. Li Y, Chen D, Jin L, Liu J, Su Z, Li Y, Gui Y and Lai Y: MicroRNA-20b-5p functions as a tumor suppressor in renal cell carcinoma by regulating cellular proliferation, migration and apoptosis. Mol Med Rep 13: 1895-1901, 2016.
12. Li D, Ilnytskyy Y, Kovalchuk A, Khachigian LM, Bronson RT, Wang B and Kovalchuk O: Crucial role for early growth response-1 in the transcriptional regulation of miR-20b in breast cancer. Oncotarget 4: 1373-1387, 2013.
13. Wang B, Yang J and Xiao B: MicroRNA-20b (miR-20b) promotes the proliferation, migration, invasion, and tumorigenicity in esophageal cancer cells via the regulation of phosphatase and tensin homologue expression. PLoS One 11: e0164105, 2016.
14. Zhu J, Chen L, Zou L, Yang P, Wu R, Mao Y, Zhou H, Li R, Wang K, Wang W, *et al*: miR-20b, -21, and -130b inhibit PTEN expression resulting in B7-H1 over-expression in advanced colorectal cancer. Hum Immunol 75: 348-353, 2014.
15. Landais S, Landry S, Legault P and Rassart E: Oncogenic potential of the miR-106-363 cluster and its implication in human T-cell leukemia. Cancer Res 67: 5699-5707, 2007.
16. Clevers H: Wnt/beta-catenin signaling in development and disease. Cell 127: 469-480, 2006.
17. Hoppler S and Kavanagh CL: Wnt signalling: Variety at the core. J Cell Sci 120: 385-393, 2007.
18. MacDonald BT, Tamai K and He X: Wnt/beta-catenin signaling: Components, mechanisms, and diseases. Dev Cell 17: 9-26, 2009.
19. Yang Z, Shah K, Busby T, Giles K, Khodadadi-Jamayran A, Li W and Jiang H: Hijacking a key chromatin modulator creates epigenetic vulnerability for MYC-driven cancer. J Clin Invest 128: 3605-3618, 2018.
20. Dejure FR and Eilers M: MYC and tumor metabolism: Chicken and egg. EMBO J 36: 3409-3420, 2017.
21. Beà S: Cyclin D1 transcriptional activation in MCL. Blood 123: 1979-1980, 2014.
22. Livak KJ and Schmittgen TD: Analysis of relative gene expression data using real-time quantitative PCR and the 2(-Delta Delta C(T)) method. Methods 25: 402-408, 2001.
23. Duan FG, Wang MF, Cao YB, Dan Li, Li RZ, Fan XX, Khan I, Lai HL, Zhang YZ, Hsiao WW, *et al*: MicroRNA-421 confers paclitaxel resistance by binding to the KEAP1 3'UTR and predicts poor survival in non-small cell lung cancer. Cell Death Dis 10: 821, 2019.
24. Ou SI, Cui J, Schrock AB, Goldberg ME, Zhu VW, Albacker L, Stephens PJ, Miller VA and Ali SM: Emergence of novel and dominant acquired EGFR solvent-front mutations at Gly796 (G796S/R) together with C797S/R and L792F/H mutations in one EGFR (L858R/T790M) NSCLC patient who progressed on osimertinib. Lung Cancer 108: 228-231, 2017.
25. Huang T, Alvarez AA, Pangeni RP, Horbinski CM, Lu S, Kim SH, James CD, J Raizer J, A Kessler J, Brenann CW, *et al*: A regulatory circuit of miR-125b/miR-20b and Wnt signalling controls glioblastoma phenotypes through FZD6-modulated pathways. Nat Commun 7: 12885, 2016.
26. Yamada N, Noguchi S, Mori T, Naoe T, Maruo K and Akao Y: Tumor-suppressive microRNA-145 targets catenin δ-1 to regulate Wnt/β-catenin signaling in human colon cancer cells. Cancer Lett 335: 332-342, 2013.
27. Trautmann M, Sievers E, Aretz S, Kindler D, Michels S, Friedrichs N, Renner M, Kirfel J, Steiner S, Huss S, *et al*: SS18-SSX fusion protein-induced Wnt/β-catenin signaling is a therapeutic target in synovial sarcoma. Oncogene 33: 5006-5016, 2014.
28. Silva J, Garcia V, Zaballos Á, Provencio M, Lombardía L, Almonacid L, García JM, Domínguez G, Peña C, Diaz R, *et al*: Vesicle-related microRNAs in plasma of nonsmall cell lung cancer patients and correlation with survival. Eur Respir J 37: 617-623, 2011.
29. Clevers H and Nusse R: Wnt/β-catenin signaling and disease. Cell 149: 1192-1205, 2012.

30. Nusse R and Clevers H: Wnt/β-catenin signaling, disease, and emerging therapeutic modalities. Cell 169: 985-999, 2017.
31. Chen Q, Cao HZ and Zheng PS: LGR5 promotes the proliferation and tumor formation of cervical cancer cells through the Wnt/β-catenin signaling pathway. Oncotarget 5: 9092-9105, 2014.
32. Shen G, Jia H, Tai Q, Li Y and Chen D: miR-106b downregulates adenomatous polyposis coli and promotes cell proliferation in human hepatocellular carcinoma. Carcinogenesis 34: 211-219, 2013.
33. Li M, Tian L, Wang L, Yao H, Zhang J, Lu J, Sun Y, Gao X, Xiao H and Liu M: Down-regulation of miR-129-5p inhibits growth and induces apoptosis in laryngeal squamous cell carcinoma by targeting APC. PLoS One 8: e77829, 2013.
34. Korinek V, Barker N, Morin PJ, van Wichen D, de Weger R, Kinzler KW, Vogelstein B and Clevers H: Constitutive transcriptional activation by a beta-catenin-Tcf complex in $APC^{-/-}$ colon carcinoma. Science 275: 1784-1787, 1997.
35. Gaspar C, Franken P, Molenaar L, Breukel C, van der Valk M, Smits R and Fodde R: A targeted constitutive mutation in the APC tumor suppressor gene underlies mammary but not intestinal tumorigenesis. PLoS Genet 5: e1000547, 2009.
36. Janssens N, Janicot M and Perera T: The Wnt-dependent signaling pathways as target in oncology drug discovery. Invest New Drugs 24: 263-280, 2006.
37. Yamada T and Masuda M: Emergence of TNIK inhibitors in cancer therapeutics. Cancer Sci 108: 818-823, 2017.